

## Supplementary Information: On the Stability Constants of Metal-Nitrate Complexes in Aqueous Solutions

Mohammadhasan Dinpajoo<sup>1, a)</sup> Greta L Hightower,<sup>2, 3</sup> Richard E Overstreet,<sup>2</sup> Lori  
A Metz,<sup>2</sup> Neil J Henson,<sup>2</sup> Niranjana Govind,<sup>1</sup> Andrew M Ritzmann,<sup>2</sup> and Nicolas E  
Uhnak<sup>2, b)</sup>

<sup>1)</sup>*Physical & Computational Sciences Directorate, Pacific Northwest National  
Laboratory, Richland WA, 99352*

<sup>2)</sup>*National Security Directorate, Pacific Northwest National Laboratory,  
Richland WA, 99352*

<sup>3)</sup>*University of Hartford, West Hartford, CT, 06117*

(Dated: February 13, 2025)

---

<sup>a)</sup>Electronic mail: hadi.dinpajoo@pnnl.gov

<sup>b)</sup>Electronic mail: nicolas.uhnak@pnnl.gov

In this supplementary material, we present additional structural and thermochemistry analyses to complement the discussions in the main text. We also provide the coordinates of the optimized structures for the studied hydrated metal complexes noting that all optimized structures have either zero imaginary frequencies or one or two negligible imaginary frequencies due to numerical errors in calculating the numerical Hessian in COSMO calculations. Further optimizations have been shown to remove these numerical errors with negligible changes in the optimized energies and structures (results not shown).

## I. STRUCTURAL ANALYSES: BOND LENGTHS, CHARGE DENSITIES, AND BOND ORDERS

Table S1 reports the average M-O bond lengths and the charge densities for both reactants and products from the optimized structures. They are obtained by dividing the actual charge of metal complexes to the molecular volumes obtained in the CSM framework in the COSMO model. Note that the average M-O bond length for the  $[\text{UO}_2(\text{H}_2\text{O})_5]^{2+}$  does not consider molecular bonds and the average bond lengths for the studied hydrated metal complexes are consistent with previous studies.<sup>1-4</sup> In addition, the M-N bond lengths between the metal and nitrogen of the nitrate ligand,  $d_{\text{M-N}}$ , in  $[\text{M}(\text{NO}_3)(\text{H}_2\text{O})_{x-1}]^{(n-1)+}$  are reported. The M-O bond distances between the one or two closest oxygen atoms of  $\text{NO}_3^-$  and the central metal atom in  $[\text{M}(\text{NO}_3)(\text{H}_2\text{O})_{x-1}]^{(n-1)+}$  are also reported as  $d_{\text{M-O}_1}$  and  $d_{\text{M-O}_2}$ .

Figure S1 shows the metal-oxygen bond lengths,  $d_{\text{M-O}}$  (metal-oxygen of the nitrate), for both generated conformations by CREST and the selected DFT optimized structures. Comparing panel A and C with panels B and D shows that the  $d_{\text{M-O}}$  distances for bidentate and monodentate conformations from CREST are greater than the ones obtained from the optimized DFT conformations indicating that xTB calculations tend to overestimate Fe-O metal distances.

Table S1: Structural analysis of the lowest energy conformations. The average M-O bond lengths,  $d_{M-O}$ , for  $[M(H_2O)_x]^{n+}$  metal complexes and the M-N bond lengths between the metal and nitrogen of the nitrate ligand,  $d_{M-N}$ , in  $[M(NO_3)(H_2O)_{x-1}]^{(n-1)+}$ . The M-O bond distances between the one or two closest oxygen atoms of  $NO_3^-$  and the central metal atom in  $[M(NO_3)(H_2O)_{x-1}]^{(n-1)+}$  are also reported as  $d_{M-O_1}$  and  $d_{M-O_2}$ . If the product conformation is monodentate, only one distance is reported. Charge densities are also reported by dividing the actual charge of metal complexes to the molecular volumes obtained in the CSM framework in the COSMO model. Note that the  $d_{M-O}$  for hydrated metal complexes does not consider the two closest O to U (molecular bonds) in  $[UO_2(H_2O)_5]^{2+}$ .

Reactants	$d_{M-O}$ [Å]	$\rho$ [e Å <sup>-3</sup> ]	Products	$d_{M-N}$ [Å]	$d_{M-O_1}$ [Å]	$d_{M-O_2}$ [Å]	$\rho$ [e Å <sup>-3</sup> ]
$[UO_2(H_2O)_5]^{2+}$	2.47	0.0189	$[UO_2(NO_3)(H_2O)_3]^+$	2.93	2.48	2.49	0.0078
$[Sr(H_2O)_7]^{2+}$	2.60	0.0148	$[Sr(NO_3)(H_2O)_5]^+$	3.07	2.65	2.65	0.0074
$[Fe(H_2O)_6]^{2+}$	2.15	0.0197	$[Fe(NO_3)(H_2O)_5]^+$	3.13	2.16	NA	0.0085
$[Fe(H_2O)_6]^{2+}$	2.15	0.0197	$[Fe(NO_3)(H_2O)_5]^+$	2.62	2.18	2.26	0.0091
$[Fe(H_2O)_6]^{3+}$	2.03	0.0325	$[Fe(NO_3)(H_2O)_5]^{2+}$	3.00	2.14	2.15	0.0178
$[Ce(H_2O)_9]^{3+}$	2.57	0.0226	$[Ce(NO_3)(H_2O)_7]^{2+}$	3.01	2.57	2.58	0.0139
$[Ce(H_2O)_9]^{4+}$	2.43	0.0322	$[Ce(NO_3)(H_2O)_7]^{3+}$	2.90	2.44	2.45	0.0221

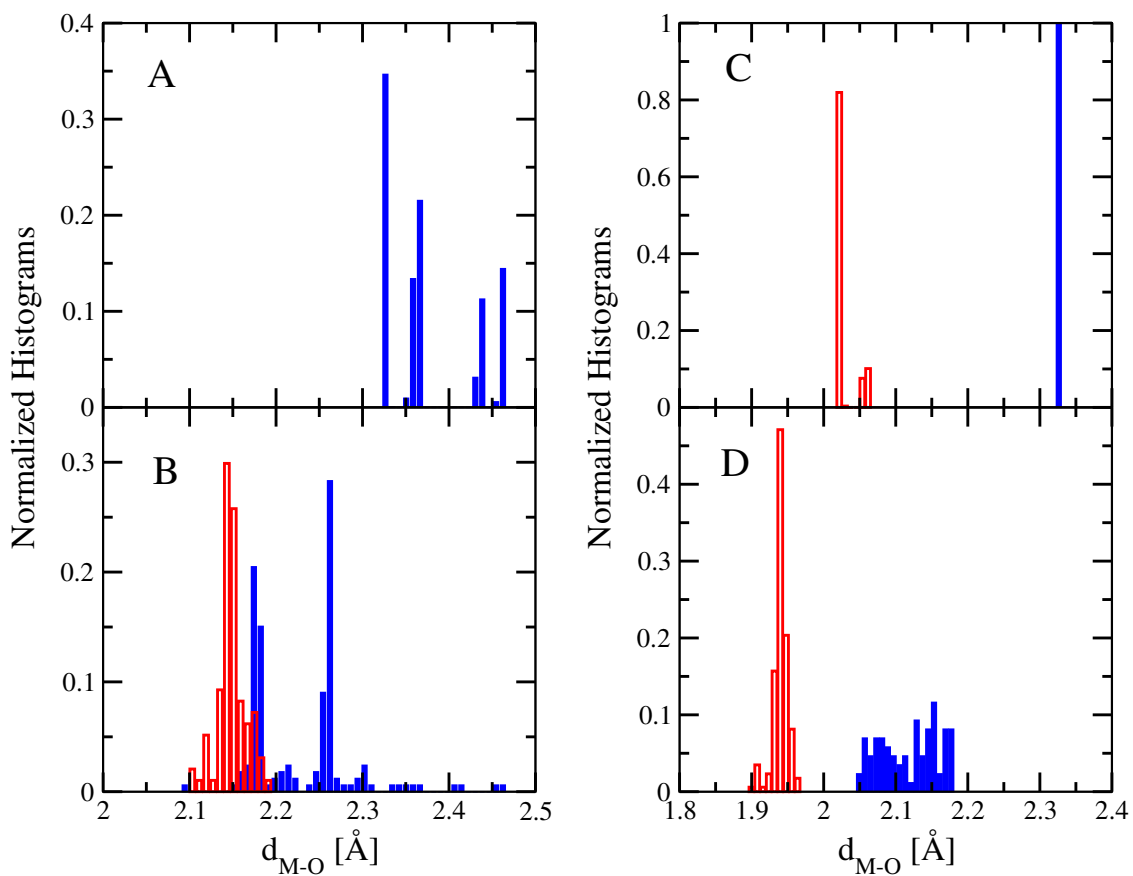


Figure S1: The metal-oxygen (MO) bond length,  $d_{M-O}$  (metal-oxygen of nitrate), distributions for monodentate (red bars) and bidentate (blue bars) conformations. A) The normalized histograms of  $d_{M-O}$  obtained from 945 generated conformations for  $[\text{Fe}(\text{NO}_3)(\text{H}_2\text{O})_5]^+$  from CREST. B) The normalized histograms of  $d_{M-O}$  obtained from 97 monodentate and 83 bidentate selected conformations for  $[\text{Fe}(\text{NO}_3)(\text{H}_2\text{O})_5]^+$  each of which are optimized at DFT. C) The normalized histograms of  $d_{M-O}$  obtained from 277 monodentate and 376 bidentate conformations for  $[\text{Fe}(\text{NO}_3)(\text{H}_2\text{O})_5]^{2+}$  generated from CREST. D) The normalized histograms of  $d_{M-O}$  obtained from 172 monodentate and 43 bidentate selected conformations for  $[\text{Fe}(\text{NO}_3)(\text{H}_2\text{O})_5]^{2+}$  each of which are optimized at DFT.

Table S2 presents the bond order analyses of metal-oxygen bond between metal and oxygen of  $\text{NO}_3^-$  in the lowest energy conformations based on the Mayer definition<sup>5</sup>. As can be seen, the bond orders of the two metal-oxygen bonds in the bidentate conformations are all almost the same except the bidentate conformation for the  $[\text{Fe}(\text{NO}_3)(\text{H}_2\text{O})_5]^+$  metal complex. This is consistent with the bond length results of the metal complexes, where only the  $[\text{Fe}(\text{NO}_3)(\text{H}_2\text{O})_5]^+$  metal complex has relatively different bond lengths.

Table S2: Bond order analysis based on the Mayer bond order analysis<sup>5</sup> of metal-oxygen bond between metal and oxygen of  $\text{NO}_3^-$  in the lowest energy conformations.

Metal-Nitrate Complex	MO type	Bond Order MO <sub>1</sub>	Bond order MO <sub>2</sub>
$[\text{Fe}(\text{NO}_3)(\text{H}_2\text{O})_5]^+$	Monodentate	0.254	NA
$[\text{Fe}(\text{NO}_3)(\text{H}_2\text{O})_5]^+$	Bidentate	0.285	0.200
$[\text{Fe}(\text{NO}_3)(\text{H}_2\text{O})_5]^{2+}$	Monodentate	0.546	NA
$[\text{Fe}(\text{NO}_3)(\text{H}_2\text{O})_5]^{2+}$	Bidentate	0.644	0.218
$[\text{Sr}(\text{NO}_3)(\text{H}_2\text{O})_5]^+$	Bidentate	0.173	0.169
$[\text{UO}(\text{NO}_3)(\text{H}_2\text{O})_3]^{1+}$	Bidentate	0.359	0.353
$[\text{Ce}(\text{NO}_3)(\text{H}_2\text{O})_7]^{2+}$	Bidentate	0.476	0.450
$[\text{Ce}(\text{NO}_3)(\text{H}_2\text{O})_7]^{3+}$	Bidentate	0.843	0.778

## II. EXAMINATION OF SPIN STATES FOR IRON COMPLEXES

In this Section, we determine the energetic differences between higher spin and lower spin states to understand how much the ground spin state is stabilized with respect to other possible spin states. This is important in the sense that if the energetic differences between ground spin state and other spin states is less than 2 kcal/mol or so, one needs to study the other spin states should because the energetic difference is within the uncertainty associated with DFT energies. We used the lowest available energy conformations at quintet/sextet states and optimized them at singlet/doublet states for  $\text{Fe}^{2+}$  and  $\text{Fe}^{3+}$  metal complexes, respectively. Table S3 tabulates the spin splitting energies defined as  $\Delta E_{HL} = E(S_H) - E(S_L)$  with  $E(S_H)$  as the energy of the lowest-energy electronic state with the high spin state  $S_H$  and  $E(S_L)$  as the energy of the lowest-energy electronic state with the low spin state  $S_L$ . As can be seen, the absolute values of the spin splitting energies between high-spin and low-spin states are more than 19 kcal/mol. Similarly, the intermediate spin state energies of  $\text{Fe}^{2+}$  (triplet) and  $\text{Fe}^{3+}$  (quartet) metal complexes have been reported in Table S3 and the energy differences between high-spin and intermediate-spin states are more than 18 kcal/mol. These results confirm that consistent with the spectroscopic series, weak ligands such as  $\text{H}_2\text{O}$  and  $\text{NO}_3^-$  result in the high spin states for Iron. Therefore, in this study we focus on the high spin states for Iron metal complexes.

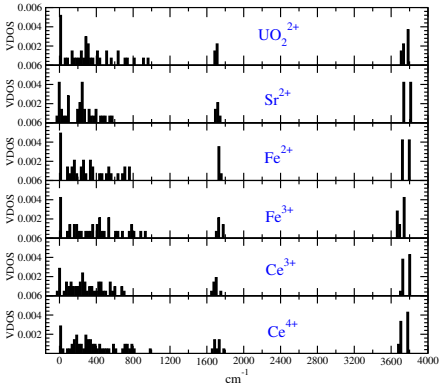
Table S3: Comparison of the energies of metal complexes with various spin states. The difference between the electronic energies of low spin and high spin metal complexes is reported in kcal/mol as

$\Delta E_{HL} = E_{\text{High spin}} - E_{\text{Low spin}}$ . Similarly, the difference between the electronic energies of intermediate spin and high spin metal complexes is reported as  $\Delta E_{HI} = E_{\text{High spin}} - E_{\text{Intermediate spin}}$ .

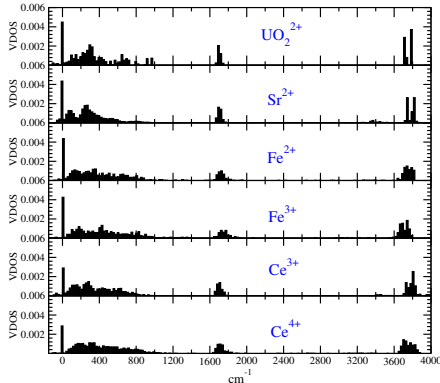
Metal Ion	Spin State	Hydrated Metal Complex	$E_{\text{tot}}$ (Hartree)	Metal-Nitrate Complex	$E_{\text{tot}}$ (Hartree)
$\text{Fe}^{2+}$	singlet ( $L$ )	$[\text{Fe}(\text{H}_2\text{O})_6]^{2+}$	-582.503	$[\text{Fe}(\text{NO}_3)(\text{H}_2\text{O})_5]^{1+}$	-786.617
$\text{Fe}^{2+}$	triplet ( $I$ )	$[\text{Fe}(\text{H}_2\text{O})_6]^{2+}$	-582.502	$[\text{Fe}(\text{NO}_3)(\text{H}_2\text{O})_5]^{1+}$	-786.620
$\text{Fe}^{2+}$	quintet ( $H$ )	$[\text{Fe}(\text{H}_2\text{O})_6]^{2+}$	-582.544	$[\text{Fe}(\text{NO}_3)(\text{H}_2\text{O})_5]^{1+}$	-786.660
			$\Delta E_{HL} \sim -26$ kcal/mol		$\Delta E_{HL} \sim -27$ kcal/mol
			$\Delta E_{HI} \sim -26$ kcal/mol		$\Delta E_{HI} \sim -27$ kcal/mol
$\text{Fe}^{3+}$	doublet ( $L$ )	$[\text{Fe}(\text{H}_2\text{O})_6]^{3+}$	-582.269	$[\text{Fe}(\text{NO}_3)(\text{H}_2\text{O})_5]^{2+}$	-786.406
$\text{Fe}^{3+}$	quartet ( $I$ )	$[\text{Fe}(\text{H}_2\text{O})_6]^{3+}$	-582.272	$[\text{Fe}(\text{NO}_3)(\text{H}_2\text{O})_5]^{2+}$	-786.409
$\text{Fe}^{3+}$	sextet ( $H$ )	$[\text{Fe}(\text{H}_2\text{O})_6]^{3+}$	-582.304	$[\text{Fe}(\text{NO}_3)(\text{H}_2\text{O})_5]^{2+}$	-786.437
			$\Delta E_{HL} \sim -22$ kcal/mol		$\Delta E_{HL} \sim -19$ kcal/mol
			$\Delta E_{HI} \sim -20$ kcal/mol		$\Delta E_{HI} \sim -18$ kcal/mol

### III. BENCHMARKING THERMAL CORRECTIONS

In this Section, we address the significance of the thermal corrections for a given ligand-exchange reaction. Figure S2 shows the normalized density of states for the hydrated metal ions,  $[M(\text{H}_2\text{O})_x]^{n+}$ . The top panel (Fig. S2A) shows the normalized density of states for the lowest minimum structure found from the procedure mentioned in Section ???. As can be seen, the lowest structures found for  $\text{UO}_2^{2+}$ ,  $\text{Fe}^{2+}$ ,  $\text{Fe}^{3+}$ , and  $\text{Ce}^{4+}$  have no imaginary frequencies while one relatively small imaginary frequency (with a magnitude of  $\approx 40 \text{ cm}^{-1}$ ) exists for  $\text{Sr}^{2+}$  and  $\text{Ce}^{3+}$ . On the other hand, the bottom panel (Fig. S2B) shows the normalized density of states for all available conformations noting that only a small percentage of the frequencies are imaginary.



(A) Normalized density of states for the lowest minimum structures of the hydrated metal ions,  $[M(\text{H}_2\text{O})_x]^{n+}$ .



(B) Normalized density of states for all minimized structures of the hydrated metal ions,  $[M(\text{H}_2\text{O})_x]^{n+}$ .

Figure S2: Density of states for the hydrated metal ions of  $\text{UO}_2^{2+}$ ,  $\text{Sr}^{2+}$ ,  $\text{Fe}^{2+}$ ,  $\text{Fe}^{3+}$ ,  $\text{Ce}^{3+}$ , and  $\text{Ce}^{4+}$  (see the main text).

To quantify the order of magnitude of error that can appear in the reaction thermodynamical properties due to the existence of imaginary frequencies for these calculations, here we focus on the reaction  $[\text{Ce}(\text{H}_2\text{O})_9]^{4+} + \text{NO}_3^{-}(\text{aq}) \rightarrow [\text{Ce}(\text{NO}_3)(\text{H}_2\text{O})_7]^{3+}(\text{aq}) + 2 \text{H}_2\text{O}(\text{aq})$ . We first find the lowest energy conformations with no imaginary frequencies using the procedure described in the main text. For the  $[\text{Ce}(\text{NO}_3)(\text{H}_2\text{O})_7]^{3+}$  species, we also find another conformation with two imaginary frequencies with a magnitude of  $144 \text{ cm}^{-1}$  and  $35$  whose electronic energy is about  $0.09 \text{ kcal/mol}$  higher in energy than the conformation with zero imaginary frequency. Table S4 reports the thermodynamical enthalpy, entropy, and

Table S4: Thermochemistry of the reaction  $[\text{Ce}(\text{H}_2\text{O})_9]^{4+}(\text{aq}) + \text{NO}_3^{-1}(\text{aq}) \rightarrow [\text{Ce}(\text{NO}_3)(\text{H}_2\text{O})_7]^{2+}(\text{aq}) + 2 \text{H}_2\text{O}(\text{aq})$  at B3LYP DFT level of theory and 298.15 K. Here for the  $[\text{Ce}(\text{H}_2\text{O})_9]^{4+}(\text{aq})$  species, we use conformations with zero and one imaginary frequencies and for the  $[\text{Ce}(\text{NO}_3)(\text{H}_2\text{O})_7]^{3+}(\text{aq})$  species, we use conformations with zero and two imaginary frequencies. The magnitude of the imaginary frequency for the conformation is  $78 \text{ cm}^{-1}$  whose electronic energy is about 0.03 kcal/mol more negative than the conformation with zero imaginary frequency. Below #IMG stands for the number of imaginary frequencies and  $\nu_{\text{cut}}$  shows the frequency below which the magnitudes of frequencies are replaced with that cutoff frequency (quasi-harmonic approximation).

#IMG	$\nu_{\text{cut}}$ ( $\text{cm}^{-1}$ )	$\Delta E_{\text{tot}}$ (kcal/mol)	$\Delta_r H$ (kcal/mol)	$T\Delta_r S$ (kcal/mol)	$\Delta_r G$ (kcal/mol)
<b>Lowest Energy Conformers</b>					
0	50	-7.6	-10.8	8.0	-18.8
2	50	-7.7	-10.9	9.0	-19.9
0	100	-7.6	-10.8	8.2	-19.0
2	100	-7.7	-10.9	8.8	-19.7
<b>24 Reactant Conformers, 21 Product Conformers</b>					
37	50	-7.6	-11.4	8.9	-20.3
37	100	-7.6	-11.4	8.6	-20.0

Gibbs free energies in the quasi-harmonic approximation when the  $[\text{Ce}(\text{NO}_3)(\text{H}_2\text{O})_7]^{3+}(\text{aq})$  has zero and two imaginary frequencies. Generally, one would expect differences in the thermal corrections for two independent configurations, but one can still evaluate and compare the thermal corrections for two independent configurations, one of which has two imaginary frequencies. Depending on the frequency cutoff used in the quasi-harmonic approximation, the deviations between the thermodynamical reaction properties involving these two configurations are observed. In particular, the differences are less than about 1.2 kcal/mol with percent errors of 1.0 %, 12.5 %, and 5.8 % in reaction enthalpy, entropy, and Gibbs free energies, respectively for a frequency cutoff of  $50 \text{ cm}^{-1}$ . Interestingly, the differences tend to decrease to about 0.7 kcal/mol with percent errors of 1.0 %, 7.3 %, and 4.7 % in reaction enthalpy, entropy, and Gibbs free energies, respectively for a frequency cutoff of  $100 \text{ cm}^{-1}$ .

The bottom section of Table S4 shows the Boltzmann average values of the reaction obtained from 24 reactant conformations and 21 product conformations. For a frequency cutoff of  $50 \text{ cm}^{-1}$ , the Gibbs free energies are about 1.5 kcal/mol more negative than the



one from the lowest energy conformations with zero imaginary frequencies noting that the enthalpies and temperature times entropies are only different by less than 1.0 kcal/mol. Smaller differences are observed for a frequency cutoff of  $100 \text{ cm}^{-1}$ , when the reaction thermodynamical properties are compared with the ones with the lowest energy conformations with zero imaginary frequencies but the differences remain by about 1.2 kcal/mol. Therefore, for these reactions, the results indicate that possible errors associated with including the imaginary frequencies within the quasi-harmonic approximation remain to be about 1.0 kcal/mol for  $\text{Ce}^{4+}$  metal complexes. We also find the errors for the iron metal complexes. The errors in the Gibbs free energies turn out to be about 0.5 kcal/mol, which is less than the ones for  $\text{Ce}^{4+}$  presented above mainly because a more comprehensive sampling are done for iron metal complexes; therefore, for the comparisons one could generally find conformations with closer energies to the lowest energy conformation (results not shown).

### A. Scaling of Frequencies in Thermal Corrections

It is common to scale the frequencies in the rigid-rotor harmonic approximation to account for the anharmonicity and other effects in an implicit way.<sup>6</sup> It is worth noting that this technique may be used to make the calculated properties have less deviation from the experimental values when they are available. Table S5 reports the effects of such scaling on the calculated thermodynamical properties for  $\text{Ce}^{4+}$  metal ions. As can be seen, the scaling of frequencies only changes the thermodynamical properties by less than 7 % when compared with no scaling. Therefore, the systematic errors are minimal in this aspect.

Table S5: Thermochemistry of reaction  $[\text{Ce}(\text{H}_2\text{O})_9]^{4+}(\text{aq}) + \text{NO}_3^{-1}(\text{aq}) \rightarrow [\text{Ce}(\text{NO}_3)(\text{H}_2\text{O})_7]^{2+}(\text{aq}) + 2 \text{H}_2\text{O}(\text{aq})$  from raw DFT calculations when the vibrational frequencies are scaled to account for anharmonic effects. The lowest energy conformation has been used for all reactants and products.

M	S	$\Delta E_{\text{tot}}$ (kcal/mol)	$\Delta_r H$ (kcal/mol)	$T\Delta_r S$ (kcal/mol)	$\Delta_r G$ (kcal/mol)
<b>Scaling Factor: 0.8</b>					
$\text{Ce}^{4+}$	1	-7.6	-10.2	7.6	-17.8
<b>Scaling Factor: 1.0</b>					
$\text{Ce}^{4+}$	1	-7.6	-10.8	8.0	-18.8
<b>Scaling Factor: 1.2</b>					
$\text{Ce}^{4+}$	1	-7.6	-11.6	8.4	-20.0

#### IV. OPTIMIZED STRUCTURES FOR $M^{n+}(\text{H}_2\text{O})_x$ METAL COMPLEXES

Unless mentioned, all the structures are optimized at B3LYP with Stuttgart 1997 RSC ECP-type basis sets. Please note that the xyz files for these optimized structures are also available as a zip file on the journal website.

Optimized structure for  $[\text{UO}_2(\text{H}_2\text{O})_5]^{2+}$ :

```
U -0.00550913 0.07477658 -0.05050331
O 0.00833979 0.08106420 1.71266518
O -0.00390407 0.06481393 -1.81303375
O -2.43724084 0.09710273 -0.11753482
H -2.89962484 -0.14657421 -0.93504455
O 2.18126615 1.20274726 -0.31510650
H 2.48258708 1.77996552 0.40516303
O -0.54291302 2.47030052 -0.04819687
H -1.05180647 2.75418427 -0.82576695
O 1.93842133 -1.52206745 -0.02707802
H 1.70797591 -2.39910445 0.31777040
O -0.63075872 -2.32741149 -0.04134021
H -1.12865695 -2.60083929 -0.82914420
H -1.17362443 -2.59850938 0.71733064
H -2.97801118 -0.25447136 0.60751202
H -1.06216068 2.75674604 0.72143971
H 2.35906630 1.68774364 -1.13659559
H 2.70546265 -1.22430536 0.48729250
```

Optimized structure for  $[\text{Sr}(\text{H}_2\text{O})_8]^{2+}$ :

```
Sr -0.06096710 -0.34907664 0.05992791
O -0.52974632 3.75384616 -0.08471546
O -0.97068503 1.54681381 1.57615014
O -1.17038870 -1.48291123 2.14245172
O -0.83277617 1.45193963 -1.66275228
O 0.94242230 -1.66996717 -1.93797844
```

O -2.09874042 -1.39245528 -1.18009702  
O 2.17864260 0.93272900 -0.26253055  
O 1.83682248 -1.73306456 1.17952601  
H -2.66690912 -0.74612754 -1.62414921  
H -2.70785338 -1.94434063 -0.66856495  
H 1.65377075 -1.27183963 -2.45972793  
H 0.32277738 -2.02597478 -2.59107902  
H 0.36561626 4.12071316 -0.03852807  
H -1.11481874 4.52463746 -0.12564731  
H -0.83217816 2.42676875 1.16842722  
H -0.59378001 1.60978312 2.46474190  
H -2.12989237 -1.35784440 2.18996571  
H -1.05201318 -2.44298445 2.19612052  
H -0.35192334 1.44795337 -2.50226742  
H -0.71648115 2.35351848 -1.29858851  
H 2.85034415 0.63573917 0.36856234  
H 2.15638755 1.89682374 -0.17459857  
H 2.27500850 -2.39000260 0.61926366  
H 1.62000364 -2.20688139 1.99520642

Optimized structure for  $[\text{Sr}(\text{H}_2\text{O})_7]^{2+}$ :

Sr -0.04005167 -0.32330301 0.05819260  
H 1.63321859 -2.21363695 1.97021632  
O -1.02684187 1.53310270 1.57922593  
O -1.15114986 -1.42954462 2.14869076  
O -0.81810941 1.46405894 -1.69956226  
O 0.93511495 -1.64806667 -1.94550884  
O -2.09617306 -1.36095284 -1.15201450  
O 2.20933917 0.93690238 -0.28307284  
O 1.85103108 -1.72965821 1.16082647  
H -2.67372705 -0.73158285 -1.60816932  
H -2.69658280 -1.90020635 -0.61708108

H 1.62868245 -1.23864310 -2.48228635  
H 0.30130710 -2.00352538 -2.58517172  
H 2.19835874 1.90115923 -0.19517352  
H 2.28811935 -2.37999179 0.59201085  
H -0.80290902 2.46187045 1.42230489  
H -0.94330841 1.41855282 2.53731599  
H -2.11252981 -1.32164042 2.20062728  
H -1.01378823 -2.38597408 2.21794412  
H -0.43725267 1.26179403 -2.56696694  
H -0.47531555 2.34418449 -1.48492510  
H 2.89414799 0.63370122 0.33058726

Optimized structure for  $[\text{Fe}(\text{H}_2\text{O})_6]^{2+}$ :

Fe 0.01353884 -0.01787850 0.00830614  
O -1.18738416 -0.20656494 1.79148323  
H -2.10375071 -0.46933243 1.61758731  
H -0.85412033 -0.84409990 2.44129441  
O 1.25503289 0.39794683 -1.69920821  
H 1.84994181 -0.32579148 -1.94955442  
H 0.76825889 0.61610728 -2.50917028  
O 1.23454150 1.25924443 1.21565974  
H 1.82003170 1.84126291 0.70627269  
H 0.72977452 1.85401519 1.79278505  
O -1.20548341 -1.40984741 -1.05764665  
H -1.86548488 -0.98851593 -1.62990535  
H -0.71966485 -2.01788397 -1.63651628  
O 1.24322209 -1.73264536 0.46728129  
H 2.07846464 -1.49627476 0.89812746  
H 0.82419453 -2.37423768 1.06120304  
O -1.24185695 1.60753599 -0.64426681  
H -1.89600508 1.90223092 0.00778893  
H -0.74314434 2.40473939 -0.88196457

Optimized structure for  $[\text{Fe}(\text{H}_2\text{O})_6]^{3+}$ :

Fe -0.11805417 0.12920538 -0.17623396  
O 1.63672387 -0.31923214 -1.09952985  
H 1.67882117 -1.14618707 -1.61189159  
H 2.04981382 0.36579190 -1.65516335  
O 0.34424453 2.09640003 -0.19950421  
H -0.21428398 2.70833547 -0.71048756  
H 0.62707565 2.56426550 0.60510462  
O 0.84954936 -0.14791135 1.59711557  
H 1.82193877 -0.09035142 1.56953779  
H 0.55787031 0.35526306 2.37779823  
O -1.87588867 0.55793298 0.75354512  
H -1.95142502 1.40434438 1.22894264  
H -2.27717161 -0.11607817 1.33077957  
O -1.07004410 0.39568156 -1.95392219  
H -0.78179842 -0.12746973 -2.72294850  
H -2.04322772 0.35065633 -1.92950550  
O -0.56502835 -1.84709471 -0.15600266  
H -0.32014937 -2.31943212 0.65934699  
H -1.46460984 -2.13268772 -0.39294423

Optimized structure for  $[\text{Ce}(\text{H}_2\text{O})_9]^{3+}$ :

Ce -0.10163274 -0.01123048 0.37754469  
O 0.86196087 1.65111735 2.10217317  
O 0.78532255 -1.66242238 2.09680534  
O -1.75847571 0.02500555 -1.58721551  
O -1.44935292 2.17226521 0.26093305  
O -1.47399558 0.00666702 2.56234751  
O -1.51683733 -2.15392447 0.18527329  
O 2.48850643 -0.07463989 0.26717425  
O 0.82181489 -1.73041949 -1.26121225  
O 0.93626203 1.65065184 -1.27949497

H 1.90196409 1.55005511 -1.25062322  
H 0.69973114 1.57960653 -2.21711617  
H -2.34404990 -2.00460349 -0.29862524  
H -1.76356725 -2.63716804 0.98830698  
H -1.31434736 0.80282702 3.09272722  
H -2.43423223 -0.01536224 2.42377503  
H 1.34970581 2.40787690 1.74284960  
H 1.43356792 1.28421199 2.79448272  
H 0.10547157 -2.12318051 2.61206486  
H 1.37991700 -2.35515344 1.77128518  
H -1.39538571 -0.25729075 -2.44080623  
H -2.12716306 0.90813944 -1.74392348  
H -1.71207198 2.57411790 1.10268552  
H -0.94712046 2.85973174 -0.20384400  
H 3.00871945 0.22262987 1.02820448  
H 2.90137015 -0.90397648 -0.01674072  
H 0.18133479 -2.41784307 -1.50057252  
H 1.27726614 -1.48758170 -2.08134174

Optimized structure for  $[\text{Ce}(\text{H}_2\text{O})_9]^{4+}$ :

Ce -0.06824587 0.01320788 0.04727800  
O -0.10355473 2.42089724 -0.41748382  
O -0.15052968 1.29294864 2.10254947  
O 1.33289870 -1.70055619 -0.99867290  
O 1.47970390 -0.88256412 1.73187121  
O -1.30030469 -1.21107985 1.73729102  
O -0.03419099 0.41539961 -2.33164494  
O -2.30952855 0.87677607 0.28130396  
O -1.50612801 -1.65033012 -0.95331867  
O 2.21171799 0.78854818 -0.31223772  
H 2.74913221 0.21187765 -0.88206862  
H 2.39309565 1.69996638 -0.59430406

H 0.77073230 0.70085202 -2.79663337  
H -0.53711542 -0.13520964 -2.95410486  
H -1.14726293 -0.97612270 2.66827447  
H -1.34263124 -2.18250903 1.69955706  
H 0.36692300 3.05048312 0.15425911  
H 0.03423227 2.72547273 -1.32967016  
H -0.75810126 2.03763861 2.24744475  
H 0.65360459 1.48391451 2.61417652  
H 1.22855132 -1.93265981 -1.93596895  
H 1.53762617 -2.52401157 -0.52454688  
H 2.42832230 -0.74993823 1.56353531  
H 1.38183846 -1.82739877 1.94382744  
H -2.63156450 1.45564259 -0.43076363  
H -3.05326528 0.31890015 0.56440329  
H -1.16753881 -2.35336332 -1.53192123  
H -2.38415599 -1.40820865 -1.29272353

**V. OPTIMIZED STRUCTURES FOR  $M^{(n-1)+}NO_3(H_2O)_x$  METAL  
COMPLEXES: B3LYP WITH STUTTGART 1997 RSC ECP-TYPE BASIS  
SETS**

Optimized structure for  $[UO_2NO_3(H_2O)_3]^+$ :

U -0.12880064 0.19256429 0.10394162  
O 0.48519797 0.26300439 1.75649629  
O -0.73544210 0.18639433 -1.55332036  
O 2.08293683 0.88279613 -0.68371748  
H 2.34552770 0.67720302 -1.59540489  
O -2.34105876 0.15745269 1.20591803  
H -2.44555262 -0.29634610 2.05731102  
O -0.55620763 2.57491284 0.20063904  
H -0.76385911 3.10432251 -0.58522628  
H -0.10696342 3.16077010 0.83008661

H 2.82304147 0.60443603 -0.12010079  
H -3.06432494 -0.15919567 0.64034567  
N 0.29067037 -2.70967101 0.02086926  
O 0.46287727 -3.90424404 -0.00711669  
O -0.79856341 -2.17705029 0.43085131  
O 1.18121577 -1.87187117 -0.35485107

Optimized structure for  $[\text{Sr}(\text{NO}_3)(\text{H}_2\text{O})_5]^+$ :

Sr -0.35187080 0.16681098 -0.09614488  
O -2.71909370 1.18543859 0.18495960  
H -3.20121644 1.40591478 -0.62541770  
H -2.80408929 1.97271973 0.74267511  
O -0.13785052 1.57742910 2.07189358  
H 0.73392396 1.64373623 2.48803579  
H -0.45299813 2.49104446 2.01065910  
O -1.51731201 -1.05280332 -2.07025221  
H -0.97632372 -1.73202609 -2.49895060  
H -2.34933898 -1.49994450 -1.85733967  
O -1.37326153 -1.67083333 1.41082673  
H -2.12804583 -1.39684768 1.95199506  
H -0.77540739 -2.11476185 2.03025304  
O 0.48651593 2.36653829 -1.17944100  
H 0.54517073 2.32802388 -2.14583853  
H 1.35036593 2.69859355 -0.89524496  
N 2.46533822 -1.05010525 -0.19473642  
O 3.61876913 -1.48582460 -0.26508775  
O 2.06703739 -0.41183689 0.82505670  
O 1.64036407 -1.22507900 -1.14107073

Optimized structure for the monodentate  $[\text{Fe}(\text{NO}_3)(\text{H}_2\text{O})_5]^+$ :

Fe 0.15651016 0.74558717 0.03040529  
O 0.11773378 2.89512956 0.01478306



H 0.92956457 3.35036254 0.28331552  
H -0.16573415 3.33409617 -0.80086259  
O 2.29481512 0.71082916 -0.25606481  
H 2.59302402 -0.09234361 -0.71142123  
H 2.62786155 1.44054208 -0.80226692  
O -1.95362609 0.67549385 0.30822270  
H -2.25858869 0.94487720 1.18742054  
H -2.10145647 -0.29694352 0.25866455  
O 0.47018078 0.82347851 2.16137476  
H -0.01082564 1.52261216 2.63046891  
H 0.22796040 0.00270635 2.61746362  
O -0.16221294 0.72952510 -2.09653873  
H 0.05901151 -0.10842726 -2.53085635  
H 0.32824172 1.40385247 -2.59116041  
N -0.49387017 -2.30538466 -0.05871586  
O -1.70812989 -1.99694192 -0.10478171  
O -0.12683599 -3.47871796 -0.15876790  
O 0.39090684 -1.39432635 0.10551510

Optimized structure for the bidentate  $[\text{Fe}(\text{NO}_3)(\text{H}_2\text{O})_5]^+$ :

Fe -0.07863341 -0.01096600 -0.43371613  
O 2.72584772 1.66564798 1.43782891  
H 3.16707848 2.48450131 1.16803734  
H 3.22836235 1.34069532 2.19944954  
O -0.76074419 1.56420117 -1.64726710  
H -1.26453166 1.25950927 -2.41852095  
H -1.33300270 2.20677554 -1.19938652  
O -0.00658270 1.40415688 1.17666455  
H -0.50381279 1.15821923 1.97046372  
H 0.91057880 1.59499572 1.47324392  
O -0.24006199 -1.20947841 -2.21708652  
H -0.73630956 -2.03699640 -2.12531495

H 0.56829249 -1.44392495 -2.69766423  
O 2.01839446 -0.15583731 -0.46807427  
H 2.46309214 -0.08864276 -1.32590805  
H 2.47323591 0.48391533 0.12800428  
N -1.59458414 -1.67509447 0.90381454  
O -0.31597106 -1.72984301 0.88373069  
O -2.26331353 -2.47309330 1.54291592  
O -2.11336799 -0.74077672 0.21828323

Optimized structure for bidentate  $[\text{Fe}(\text{NO}_3)(\text{H}_2\text{O})_5]^{2+}$ :

Fe 0.48500980 0.02083632 0.02305512  
O 2.64221859 0.09274315 0.13335354  
H 3.12192245 -0.73272323 -0.04872480  
H 3.06118500 0.76720654 -0.42732015  
O 0.56580572 1.93052471 -0.69398807  
H 0.19634066 2.04656075 -1.58629549  
H 0.13692919 2.60013486 -0.13352547  
O 0.55897945 -1.90303673 0.72853811  
H 0.14387661 -2.57127640 0.15677229  
H 0.18424707 -2.03785838 1.61597744  
O 1.01011728 -0.76916485 -1.85815279  
H 1.90216623 -0.56483549 -2.18254152  
H 0.40853208 -0.54435601 -2.58770831  
O 0.93483708 0.70532605 1.94886408  
H 1.83322426 0.47371566 2.23638763  
H 0.33509644 0.44848212 2.66896283  
N -2.08958237 0.01752706 -0.01624322  
O -1.35841830 -0.38923616 -0.98688768  
O -3.28772915 0.01573652 -0.04101500  
O -1.39966703 0.42567221 0.98151586

Optimized structure for  $[\text{Fe}(\text{NO}_3)(\text{H}_2\text{O})_4]^+$ :

Fe 0.26480630 0.79365017 0.07280937

O 0.39029045 2.89430199 0.09591919  
H 1.22942633 3.23235845 0.44613844  
H -0.30086602 3.34893499 0.60271858  
O 2.39246671 0.74437351 -0.07136419  
H 2.82400472 1.01068104 -0.89677387  
H 2.83088108 -0.07568558 0.20032310  
O -1.86115878 0.96891896 0.25026499  
H -2.32906137 0.17526330 0.55073639  
H -2.36358301 1.29502479 -0.51165518  
O 0.38678911 0.46242988 2.24761717  
O 0.29821710 -1.54703574 3.10415005  
O 0.19760823 -1.24484253 0.94255317  
O 0.06715037 0.23357932 -1.95248169  
H -0.75140167 -0.23369758 -2.18401179  
H 0.78294873 -0.31555772 -2.31093161  
N 0.29434978 -0.80424333 2.13343221

Optimized structure for  $[\text{Fe}(\text{NO}_3)(\text{H}_2\text{O})_4]^{2+}$ :

Fe 0.26069641 0.77345041 0.15080178  
O 0.14180266 2.80819581 0.19288850  
H -0.11575739 3.19643776 1.04892205  
H -0.45242622 3.20930973 -0.46733245  
O 2.21913315 1.01277882 -0.33641273  
H 2.78620513 1.47359420 0.30597388  
H 2.69476193 0.20767255 -0.60743977  
O -1.77152763 0.66417061 0.35625631  
H -2.14229286 -0.18756840 0.64755691  
H -2.16185691 1.33598340 0.94322428  
O 0.62899651 0.61986730 2.18897592  
O 0.91369861 -1.36133576 3.07904077  
O 0.52759751 -1.11763713 0.93593191  
O -0.05450933 0.22609474 -1.77231537

H 0.63882724 -0.29085494 -2.22119925  
H -0.89926723 -0.20208401 -1.99805676  
N 0.70425473 -0.66664263 2.13584066

Optimized structure for  $[\text{Ce}(\text{NO}_3)(\text{H}_2\text{O})_7]^{2+}$ :

Ce 0.37720183 -1.34592890 0.30647894  
O 2.10219489 0.07632431 1.52353400  
O -0.67370177 -3.36124718 -0.96713657  
O -0.92391237 -2.87178546 1.91358019  
O 2.06585436 -3.06357559 1.27796677  
O -0.62522189 -0.06073427 2.25504742  
O 2.47293696 -1.73231537 -1.09611292  
O -2.16050632 -0.98680178 -0.09724632  
H -2.52249919 -1.16855435 -0.97773597  
H -2.50942040 -0.11436448 0.13808024  
H -0.70244289 0.90335877 2.18296732  
H -1.48182660 -0.36403640 2.59246296  
H 1.86681305 -3.99469471 1.09372324  
H 2.09375427 -3.00777546 2.24673086  
H 3.03594185 -0.11995761 1.35073548  
H 2.02911779 0.12144544 2.48987283  
H 0.00649326 -4.00452084 -1.22355309  
H -1.14276225 -3.16026278 -1.79127775  
H -1.21288611 -3.68232029 1.46691712  
H -0.44870283 -3.16895154 2.70451190  
H 2.71400793 -0.99592832 -1.67883504  
H 3.28058282 -1.96835505 -0.61524983  
N -0.01207134 0.68887757 -1.87439487  
O 0.11172800 1.02429193 -0.65219415  
O 0.08707748 -0.55406243 -2.13145870  
O -0.21698669 1.51307583 -2.75133116

Optimized structure for  $[\text{Ce}(\text{NO}_3)(\text{H}_2\text{O})_7]^{3+}$ :

Ce 0.25713284 0.19436569 0.08453842  
 O 1.91330111 1.78929183 -0.80043490  
 O -0.96879965 1.50517915 1.74844091  
 O -0.14876183 -1.10219559 2.09798857  
 O 0.17211438 -0.10617428 -2.33510494  
 O 1.91481710 0.81706642 1.72205679  
 O -0.83891726 2.08803748 -1.02326137  
 O 2.19265990 -1.14106685 -0.43535575  
 H 2.31176981 1.69832762 1.61625607  
 H 1.72833325 0.70540250 2.66958797  
 H 0.66273589 0.42576679 -2.98161042  
 H -0.08858024 -0.92783751 -2.78024152  
 H 1.49945653 2.47621138 -1.35090814  
 H 2.63814406 1.41985998 -1.33228201  
 H -0.67796250 2.40527289 1.97126744  
 H -1.94129153 1.51917213 1.76719228  
 H -0.69447745 -0.78788375 2.83577846  
 H -0.16981801 -2.07293123 2.10894676  
 H -1.29024674 1.87107497 -1.85624647  
 H -1.44583768 2.65438526 -0.51962919  
 H 2.17638152 -1.73816126 -1.20197581  
 H 2.61211377 -1.63650596 0.28879376  
 N -1.81701286 -1.75542495 -0.45281323  
 O -0.56419911 -2.01970939 -0.52662138  
 O -2.66901425 -2.57638570 -0.63780689  
 O -2.07038921 -0.53424114 -0.16454768

## VI. OPTIMIZED STRUCTURES FOR VARIOUS METAL COMPLEXES AT BLYP OR PBE WITH STUTTGART 1997 RSC ECP-TYPE BASIS SETS

Optimized structure for  $[\text{UO}_2(\text{H}_2\text{O})_5]^+$  obtained at BLYP:

U -0.03721949 0.12538804 -0.03201959

O -0.01869919 0.10172436 1.76642724  
O -0.05080997 0.14183643 -1.83124964  
O -2.48619433 0.27953316 0.06761085  
H -2.96430416 0.54282138 -0.74684844  
O 2.22263699 1.12747771 0.23055453  
H 2.41973161 1.62362070 1.05249295  
O -0.49207346 2.54345818 -0.01558083  
H -1.01294235 2.86585273 -0.78184779  
O 1.87399069 -1.54185991 -0.21868495  
H 2.65320867 -1.25127345 0.29956878  
O -0.74029384 -2.27226225 -0.04621785  
H -1.23595631 -2.53486655 -0.85098184  
H -1.31467950 -2.52617006 0.70741665  
H -2.86786458 0.83186362 0.78209971  
H -0.98690460 2.84110742 0.77768149  
H 2.54215352 1.69281753 -0.50417796  
H 1.63289378 -2.42644519 0.12723699

Optimized structure for  $[\text{UO}_2\text{NO}_3(\text{H}_2\text{O})_3]^+$  obtained at BLYP:

U -0.13563291 0.21651486 0.10837488  
O 0.49704513 0.29789628 1.79415862  
O -0.75903225 0.21841612 -1.58342965  
O 2.09696440 0.88168395 -0.70700346  
H 2.34863022 0.60650146 -1.61381044  
O -2.37351705 0.13379878 1.20364394  
H -2.46072941 -0.34478636 2.05438554  
O -0.56192239 2.61420398 0.22079645  
H -0.75520920 3.14435183 -0.57988233  
H -0.07101162 3.19693010 0.83650985  
H 2.83516543 0.59382693 -0.12913777  
H -3.08392443 -0.21801328 0.62632217  
N 0.29612129 -2.71203079 0.02752892

O 0.47345628 -3.92267024 0.00397998  
O -0.81566544 -2.16662790 0.43578770  
O 1.19995671 -1.85451768 -0.35150313

Optimized structure for  $[\text{UO}_2(\text{H}_2\text{O})_5]^+$  obtained at PBE:

U -0.04768251 0.07974707 -0.17695593  
O -0.03044998 0.03862757 1.60416160  
O -0.09060606 0.11834101 -1.95753157  
O -2.47405511 0.22015723 0.07216440  
H -3.01760381 0.52739638 -0.68173530  
O 2.08574599 1.30584596 0.16241741  
H 2.57221204 1.51525721 -0.66095311  
O -0.54552765 2.47898080 -0.19634583  
H -1.02000000 2.77280872 0.60845470  
O 1.83521688 -1.49046771 -0.61912140  
H 2.36846976 -1.77195273 0.15182133  
O -0.82057324 -2.25619722 -0.04779338  
H -0.64489501 -2.71881422 0.79648458  
H -0.45352518 -2.84953183 -0.73457372  
H -2.77115876 0.75179199 0.83889274  
H -1.10139876 2.78251827 -0.94338487  
H 2.73549506 0.85754273 0.74028652  
H 2.48256520 -1.16350780 -1.27598551

Optimized structure for  $[\text{UO}_2\text{NO}_3(\text{H}_2\text{O})_3]^+$  obtained at PBE:

U -0.06851044 0.11737734 0.03339544  
O -0.02932660 0.11661562 1.81920680  
O -0.09205920 0.14639454 -1.75284056  
O 2.30488698 0.74298466 0.01868283  
H 2.58622462 1.26096029 -0.76326174  
O -2.48790565 0.02830103 0.24887230  
H -3.05241847 -0.35374052 -0.45334390

O -0.54783308 2.50529826 0.04840151  
H -1.06692222 2.83240508 -0.71506777  
H -1.03868638 2.80571815 0.84112865  
H 2.59320707 1.26712941 0.79394675  
H -2.83031029 -0.34407917 1.08654535  
N 0.40340786 -2.78007067 -0.06101058  
O 0.60575875 -3.98034800 -0.10377784  
O -0.77939021 -2.26898049 -0.02602554  
O 1.35815446 -1.91019469 -0.04658253

## VII. OPTIMIZED STRUCTURES FOR VARIOUS METAL COMPLEXES AT B3LYP WITH LANL2DZ ECP-TYPE BASIS SETS

Optimized structure for  $[\text{UO}_2\text{NO}_3(\text{H}_2\text{O})_3]^+$ :

U -0.08066679 0.07428824 -0.06327022  
O -0.05737363 0.06058722 1.69769581  
O -0.11392136 0.10416802 -1.82456916  
O -2.55529608 -0.01063550 0.05504917  
H -3.06987391 -0.41888205 -0.65907906  
O 2.10708684 1.28566029 0.28362817  
H 2.40260722 1.85672685 -0.44368125  
O -0.65051543 2.49141271 -0.09088636  
H -0.35163130 3.05914039 0.63720720  
O 1.99840996 -1.36053794 -0.39426300  
H 1.87566893 -2.30190661 -0.19544890  
O -0.60983926 -2.36506215 -0.07860880  
H -1.15175966 -2.66158385 0.67082858  
H -1.09329978 -2.64361250 -0.87349663  
H -2.94466371 -0.34443967 0.87864669  
H -0.47352679 2.99482816 -0.90111421  
H 2.17837902 1.82526982 1.08708703  
H 2.74533264 -1.06399504 0.14855331



Optimized structure for  $[\text{UO}_2\text{NO}_3(\text{H}_2\text{O})_3]^+$ :

```
U -0.17626432 0.18277976 0.15704256
O -0.12032395 0.18249417 1.92092649
O -0.19328831 0.20209340 -1.60923339
O 2.22691663 0.81865204 0.11296690
H 2.71621195 0.65185373 -0.70849703
O -2.62970428 0.06187092 0.45699838
H -3.20248345 -0.30219882 -0.23659099
O -0.69903239 2.60316709 0.16553470
H -1.17614002 2.90400422 0.95596136
H -1.21637607 2.92479904 -0.59077170
H 2.79967027 0.48947326 0.82398899
H -2.91531951 -0.36254847 1.28181237
N 0.35240626 -2.74822557 0.10913334
O 0.57215244 -3.93907905 0.09606713
O -0.82770185 -2.26710178 0.14642129
O 1.28756143 -1.87792147 0.08682598
```

## REFERENCES

- <sup>1</sup>P. Nichols, E. J. Bylaska, G. K. Schenter, and W. de Jong, *J. Chem. Phys.* **128**, 124507 (2008).
- <sup>2</sup>I. Persson, *Pure Appl. Chem.* **82**, 1901 (2010).
- <sup>3</sup>C. A. Buchanan, D. Herrera, M. Balasubramanian, B. R. Goldsmith, and N. Singh, *JACS Au* **2**, 2742 (2022).
- <sup>4</sup>D. Mejia-Rodriguez, A. A. Kunitsa, J. L. Fulton, E. Aprà, and N. Govind, *J. Phys. Chem. A* **127**, 9684 (2023).
- <sup>5</sup>I. Mayer, *Chem. Phys. Lett.* **97**, 270 (1983).
- <sup>6</sup>J. R. Rustad and E. J. Bylaska, *J. Am. Chem. Soc.* **129**, 2222 (2007).